JOURNAL OF MATERIALS SCIENCE 30 (1995) 3773–3781

A fracture test using concentrically loaded square plates

K. M. ENTWISTLE
University of Manchester/UMIST, Materials Science Centre, Manchester M1 7HS, UK

A fracture test is described in which square plates are supported near their corners and loaded concentrically. The maximum tensile stress occurs on the loading circle but appreciable tensile stresses exist at the mid-point of the plate edges. To minimize premature fracture here, due to edge damage in the plate, it is desirable to reduce the ratio edge stress: maximum stress in the plate. This can be achieved by moving the points of support inwards from the plate corners to the plate centre. A justification is presented for positioning the supports on a circle of diameter d_s, where $d_s/2a=0.85$ and $2a$ is the length of the side of the plate. Loading diameters d_l of values $d_l/2a=0.25$ and $d_l/2a=0.075$ are recommended. If the plates are thin conditions can be geometrically non-linear at the fracture load. In these circumstances membrane stresses develop in addition to the pure bending of the linear regime. Calculation of the relation between the load and the stresses in the plate must then be carried out, for example by the finite element method, for the specific conditions given in the test. However, this paper demonstrates that there is a useful range of conditions under which geometrical linearity persists up to the point of fracture. Under these circumstances it is shown that it is possible to generalize the relationship between the applied load at fracture and the plate stress distribution. This permits the fracture stress to be determined from the fracture load. The procedure for doing this is set out. It is also shown how, from the fracture load of the plate, the loading geometry and the elastic constants of the material can be established if it is permissible to use the linear solution to analyse the test. It is felt that this procedure might be helpful where there is no access to either finite element packages or to finite element expertise. The finite element packages used in the work now described in this paper are ABAQUS and LUSAS.

1. Introduction

It has been demonstrated [1, 2] that useful fracture data on brittle materials can be secured by applying concentric loading to specimens in the form of square plates. The loading arrangement is illustrated in Fig. 1. The plate is supported near each corner by spheres resting in orthogonal "V" grooves in a substantial metal plate. The spheres rotate freely in the radial direction and in consequence the supports impose little constraint to the radial movements of the plate associated with its deformation under load. The load is applied through a neoprene o-ring which carries a plate with a sphere at its centre. This arrangement ensures that the load is uniformly distributed round the circumference of the o-ring. This testing arrangement has been used to obtain fracture data for alumina [1] and float glass [2].

The objective of this paper is to provide data, for those who wish to use this loading system for fracture studies, that relates the measured fracture load to the stresses in the plate at the location of the fracture origin. This is not a straightforward exercise because conditions are encountered in thin plates which are geometrically non-linear. This is the case when the deflection at the plate centre becomes comparable with the plate thickness. Under these circumstances the pure bending stresses that arise when the deflections are small have membrane stresses superimposed upon them. In this regime the relation between applied load and stresses in the plate becomes a complex function of plate geometry. It is unrealistic to hope to generalize the load–stress relations under these conditions and in practice it is necessary to perform calculations, commonly by the finite element method, for the specific conditions of individual cases. In contrast, however, if the conditions are geometrically linear useful generalizations can be made, as will be demonstrated, which permit measured fracture loads to be related to fracture stress provided that the tests are carried out in the geometrically linear regime. It is shown that it is possible to establish, for a particular loading geometry and material, if the conditions will be geometrically linear up to the point of fracture and if, therefore, the data provided here can be used with confidence to deduce the fracture stress. It turns out that geometrically linear conditions exist over a useful

0022–2461

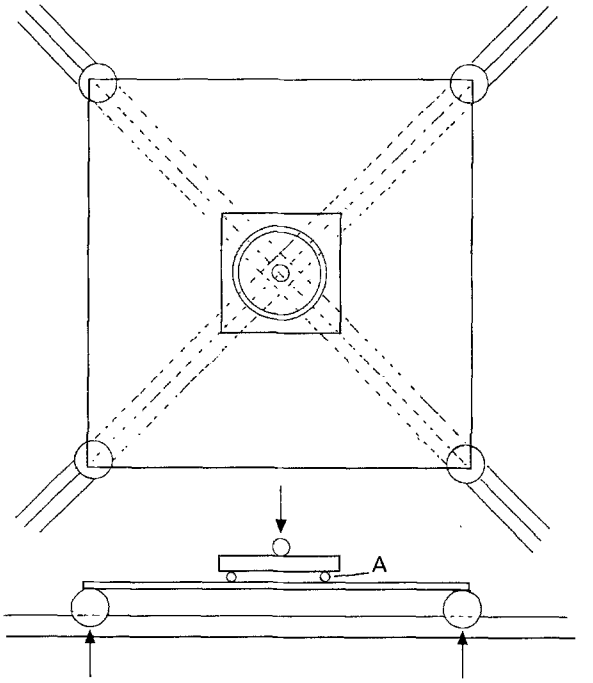

Figure 1 Diagram showing the supporting and loading arrangements for the plate. A is a neoprene o-ring. The supports are shown at the extreme corners of the plate. They are moved radially towards the plate centre for fracture stress measurement.

range of testing parameters. So it is hoped that the data now provided will be helpful to those who do not have access to finite element expertise or to finite element packages but who wish to use the testing system now described for fracture measurements. Additionally, the data may be of interest to those concerned with stresses in and deflection of concentrically loaded square plates in other contexts.

2. A comparison between the measured and the calculated stresses and deflections in loaded plates

The stresses and deflections in the loaded plates were calculated by the finite element method. The ABAQUS and the LUSAS packages were used. The element meshes for a quarter of the plate are illustrated in Fig. 2 for the LUSAS case; the ABAQUS meshes were the same as those illustrated in Ref. [1]. Geometrically linear solutions were obtained using both LUSAS and ABAQUS, and showed excellent agreement. All the geometrically non-linear calculations were carried out with ABAQUS.

Since the finite element method yields approximate solutions, it is desirable to gauge the level of approximation by comparing the solutions with directly measured values. Such a comparison has already been published for the geometrically non-linear deformation of loaded thin alumina plates [1]. The agreement between the measured and the calculated values generated confidence in the finite element data.

The comparison is now extended to measurements in the linear region on an aluminium alloy plate 254 mm square and 9.82 mm thick. The corner supports lay on a circle 350 mm in diameter, with the centre of the support circle coincident with the centre

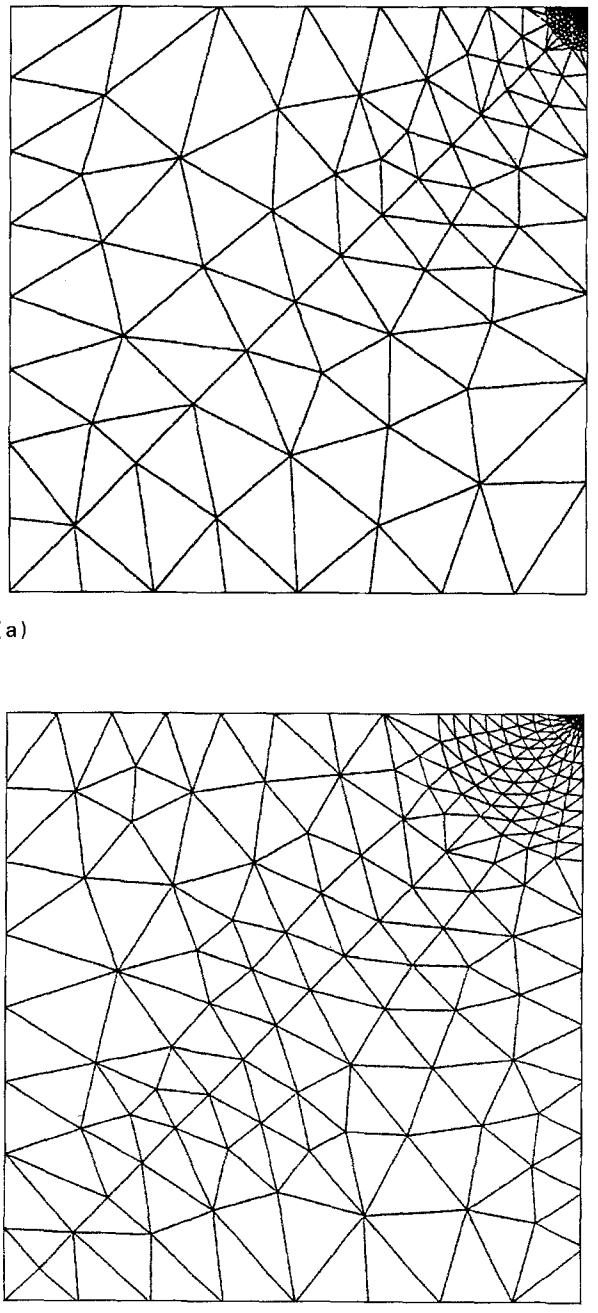

Figure 2 The LUSAS meshes for stress and displacement analysis. The mesh for a quarter of the plate is drawn. (a) The mesh for a loading circle diameter of $d_1/2a = 0.075$; (b) the mesh for a loading circle diameter of $d_1/2a = 0.25$; $2a$ is the length of the side of the plate.

of the plate. This places the corner supports 4.6 mm from the plate corners. Stress measurements were made with foil strain gauges with a gauge length of 1 mm at points on the lower (tensile) surface of the plate defined in Fig. 3. Stresses were derived from strains measured at a load of 1000 N, which produced a deflection at the centre of the plate of <0.4 mm, which is ca. 4% of the plate thickness. It is revealed later that this is well within the geometrically linear range.

In order to translate the measured strains into stress (and for the finite element calculations) a value for Young's modulus and for Poisson's ratio are required. The plate was made of duralumin (Al; 4.4 wt % Cu;

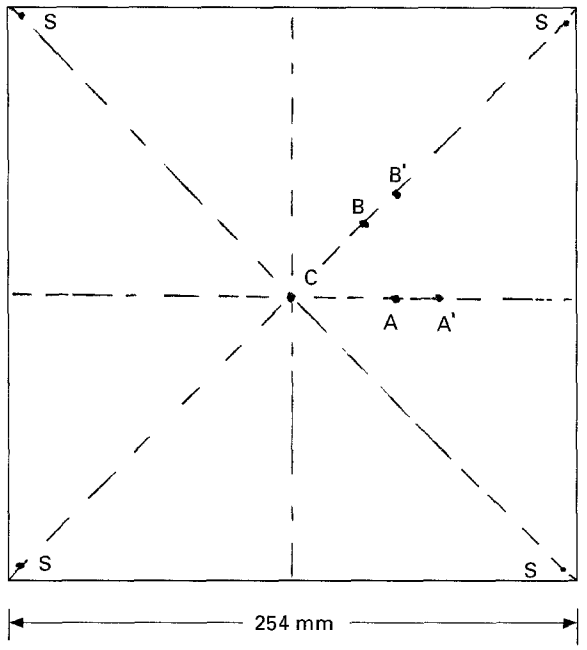

Figure 3 Diagram showing the location of the points on the lower surface of the 254 mm square duralumin plate at which the stress was measured. The coordinates of the points are: C (the plate centre) (0, 0); A (46.0, 0); A′ (65.0, 0); B (32.5, 32.5); B′ (46.0, 46.0), where the dimensions are in mm. The four points S are the supports.

TABLE I Deflection at the centre of a 254 mm square plate, 9.82 mm thick, loaded on a 19 mm diameter circle and supported at four points 4.6 mm from the plate corners: load, 1000 N

$E = 71\,500\,\mathrm{N\,mm^{-2}}$	$\nu = 0.33$
Measured deflection at centre	0.356 mm
Calculated by LUSAS	0.357 mm
Calculated by ABAQUS	0.360 mm

1.0 wt % Mg; 0.75 wt % Mn; 0.4 wt % Si). Table I shows that good agreement is obtained between the measured plate deflection and calculated values from two finite element packages using $E = 71\,500\,\mathrm{N\,mm^{-2}}$ and $\nu = 0.33$. These values are very close to published values of $E = 70\,500\,\mathrm{N\,mm^{-2}}$ and $\nu = 0.35$ [3] measured by Bradfield. The former values are used to analyse the data now described.

Table II gathers together the calculated and the measured stresses at the five locations defined in Fig. 3. The stresses are the radial stress (σ_{rr}) and the circumferential stress ($\sigma_{\theta\theta}$) which, because all the measurement points lie on lines of symmetry, are principal stresses. Table II gives data for two loading circle diameters: one of 19 mm, corresponding to $d_l/2a = 0.075$ and one of 63.5 mm diameter, corresponding to $d_l/2a = 0.25$. The diameter of the loading circle is d_l and $2a$ is the length of the side of the plate. Two sets of calculated stresses are listed, one using the ABAQUS package and the other the LUSAS package. The data for both loading circles show very satisfactory agreement between the measured and the calculated values and between the two sets of calculated stresses. The average difference between the measured and calculated stresses is ca. 4%. This level of agreement, coupled with the measurements on alumina plates previously reported [1], supports the conclusion that both the ABAQUS and the LUSAS packages, using the meshes described, give an adequate prediction of the stress distribution in the concentrically loaded square plates that are of concern here.

3. Recommended geometry for the fracture test

If the square plate is supported at its extreme corners, the tensile stress in the middle of the edge of the plate is over 80% of the maximum stress in the plate for $d_l/2a = 0.25$. All ceramic plates are likely to have some edge damage so, under this loading geometry, fracture is likely to be nucleated at the plate edge, rather than in the body of the plate. Fortunately, the probability of edge fracture can be reduced to an acceptable level by moving the corner supports radially inwards towards the plate centre. This reduces the ratio of the maximum tensile edge stress to the overall maximum tensile stress in the plate.

Table III lists this stress ratio for two loading circle diameters $d_l/2a = 0.25$ and 0.075, and for four values

TABLE II Stresses in the radial and circumferential directions at locations defined in Fig. 3 in a 254 mm square duralumin plate, 9.82 mm thick, supported at four points lying on a circle 350 mm diameter. Load, 1000 N; E, $71\,500\,\mathrm{N\,mm^{-2}}$; ν, 0.33; stresses in $\mathrm{N\,mm^{-2}}$

Location	Measured stress		Calculated stress – ABAQUS		Calculated stress – LUSAS	
	σ_{rr}	$\sigma_{\theta\theta}$	σ_{rr}	$\sigma_{\theta\theta}$	σ_{rr}	$\sigma_{\theta\theta}$
Loading circle diameter 19 mm ($d_l/2a$=0.075)						
Centre	22.90	22.90	22.27	22.27	22.29	22.29
A	9.75	14.54	9.72	14.25	9.65	14.00
B	11.73	13.21	10.96	12.79	10.98	12.92
A′	7.79	13.04	6.62	12.67	6.84	12.48
B′	9.37	10.28	9.20	9.84	9.13	10.15
Loading circle diameter 63.5 mm ($d_l/2a$=0.25)						
Centre	14.91	14.93	14.25	14.25	14.25	14.25
A	9.62	13.39	10.27	13.40	10.31	13.22
B	12.19	12.97	11.98	12.26	11.65	12.29
A′	7.29	12.23	6.97	12.23	7.10	12.04
B′	9.52	9.96	9.35	9.35	9.43	9.72

TABLE III Ratio of maximum edge stress to the maximum stress in the plate for different corner support positions ($d_s/2a$) and for two loading circle diameters ($d_l/2a$)

$d_l/2a$	Diameter of corner support circle ($d_s/2a$)			
	1.378	1.000	0.85	0.70
0.075	0.545	0.400	0.315	0.225
0.250	0.819	0.656	0.550	0.417

of the diameter of the circle on which the four supports lie, d_s, expressed in terms of the length of the side of the plate, $2a$.

Experience with glass plates [2] has shown that if the ratio of edge stress to maximum stress is ca. 0.5 a statistically acceptable proportion of a batch of plates will fail at locations away from the plate edge. Table III shows that for $d_l/2a = 0.25$ (the more critical case) a value of $d_s/2a = 0.85$ achieves this value. With this support position and a loading ring diameter of $d_l/2a = 0.075$ the stress ratio is 0.315, so edge fracture is much less likely.

It is therefore recommended that, for fracture testing, the square plates be supported at four points lying on a circle of diameter equal to 0.85 times the length of the side of the plate.

Loading circle diameters of $d_l/2a = 0.25$ and 0.075 are convenient values, and data for fracture with these loading circle sizes can be used to assess the effect of stressed volume on the average fracture stress. Data are given later that relate the load to the tensile stress distribution for these experimental conditions.

4. Defining the range of geometrical linearity

Fig. 4 illustrates the geometrically non-linear behaviour in the plate. It shows how the stresses at the centre of the plate on the bottom (tensile) and top (compressive) faces vary with applied load. The centre stress is quite close to the maximum stress in the plate. For comparison the linear solution is graphed.

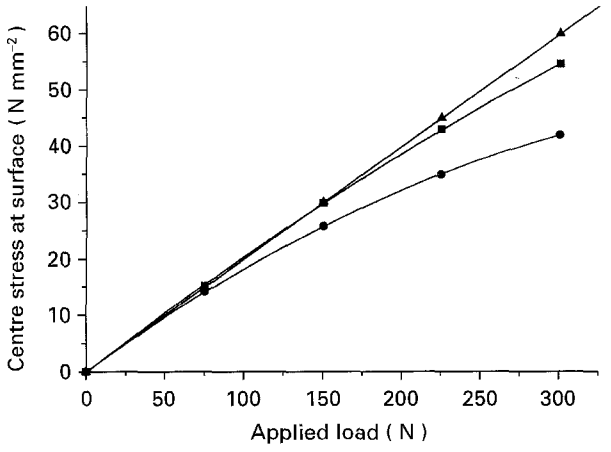

Figure 4 The calculated variation with applied load of the stresses on the lower (■) and upper (●) surface of the plate. ■ and ● are values taking account of geometrical non-linearity; ▲, linear solution. Calculated for a plate 254 mm square, thickness 2.62 mm, with $d_l/2a = 0.25$ and $d_s/2a = 1.378$; $E = 71\,500\,\mathrm{N\,mm^{-2}}$; $\nu = 0.33$.

Two features of Fig. 4 call for comment. The first is that the compressive stress on the upper plate surface falls increasingly below the tensile stress on the lower surface as the applied load increases and the plate deflection becomes larger. So conditions steadily diverge from pure bending and a tensile membrane stress develops. The second feature is that the tensile stress keeps close to the values given by the geometrically linear solution, well above the load at which the non-linear tensile and compressive stresses have begun to diverge significantly. Since compressive stresses contribute little to fracture probability they can be ignored in fracture analysis. We need to take account only of tensile stresses, and since fracture is initiated generally at the plate surface it is the surface tensile stresses that dominate fracture behaviour.

It is judged that, for analysis of the fracture test, a reasonable upper limit for the error in the tensile stress would be 2%. By this criterion it would be acceptable to use the linear finite element solution for the stress in the plate if the difference between the predictions of the linear and the non-linear analysis for the surface tensile stresses did not exceed 2%. That limit is indicated, as an example, in Fig. 4 and corresponds to a deflection at the centre of the plate (δ_c) of $\delta_c/t = 1.07$, where t is the plate thickness.

Timoshenko and Woinowsky-Krieger [4] give a simple and effective illustration of the source of geometrical non-linearity by considering the bending of a circular plate by a constant edge moment (see Fig. 5). The plate has a thickness t and an initial plan radius r. The edge moment deflects the plate into the cap of a sphere of radius of curvature R and central deflection δ. If the neutral plane is to be unchanged in length, as it would be in pure bending, the radius of a thin ring of material at the edge of the plate must be reduced from r to r'. The fractional reduction of the circumferential length of the ring will be the same as the fractional reduction of r, so a compressive hoop

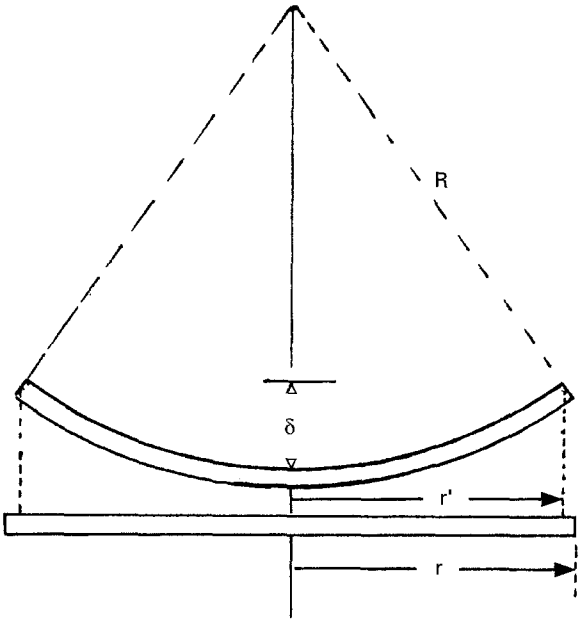

Figure 5 Diagram illustrating the development of membrane strains in the bending of a circular plate.

strain will be generated in the disc edge which will be a membrane strain, $\varepsilon_m = (r - r'/r)$. The maximum bending strain superimposed on this will be $\varepsilon_b = t/2R$.

An analysis of the geometry of Fig. 5 leads to the conclusion that

$$\frac{\varepsilon_m}{\varepsilon_b} = \frac{2\delta}{3t}$$

The development of ε_m is a consequence of the geometrical non-linearity and is seen to depend on the ratio δ/t.

In practice, elastic strains will cause the neutral axis to change its length so $(2/3)(\delta/t)$ overestimates the membrane strain. But the analysis leads to the conclusion that the onset of significant membrane stress, i.e. the onset of geometrical non-linearity, will be related to the value of δ_c/t for the plate. So a wider exploration has been made of the effect of the loading geometry of the concentrically loaded plates on the value of δ_c/t at which the linear and non-linear solutions for the tensile stress at the centre of the plate differ by 2%.

Fig. 6 summarizes the results. It records the result of finite element calculations on an aluminium alloy plate 2.62 mm thick, 254 mm square with a loading circle diameter of 63.5 mm (corresponding to $d_l/2a = 0.25$) for a range of corner support positions. Plotted are the values of the central deflection of the plate, for a range of values of $d_s/2a$, at which the linear solution for the tensile stress at the centre of the plate exceeds the non-linear solution by 2%. That deflection becomes smaller as the points of support move inwards towards the plate centre. For the support positions recommended for fracture testing, $d_s/2a = 0.85$, the value of δ_c/t at the 2% limit is 0.51. This leads to the recommendation that, provided the linear finite element solution gives a deflection at the centre of the plate less than half the plate thickness, the linear solution can be used to analyse fracture tests. Data for $d_l/2a = 0.075$ in the region of $d_s/2a = 0.85$ are also plotted. Conditions for this loading circle diameter are seen to be less critical. δ_c/t is seen to be nearly 0.6 at the 2% limit.

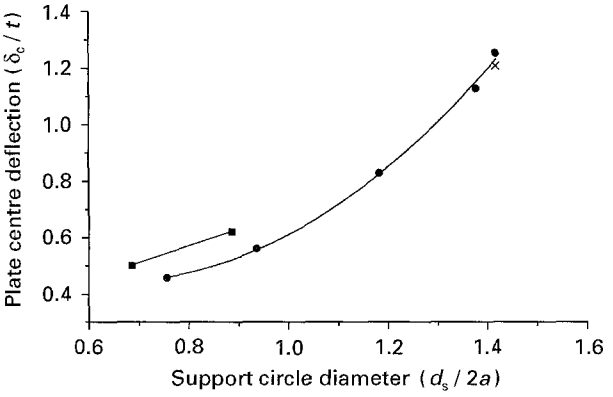

Figure 6 Plots showing the values of the deflection at the centre of the plate, normalized on the plate thickness, at which the difference between the linear and the geometrically non-linear solutions for the stress at the centre reaches 2%. Values are shown as a function of the position of the plate supports ($d_s/2a$) and for two values of the loading circle diameter ($d_l/2a$). Calculations were carried out for a plate 254 mm square and 2.62 mm thick; with $E = 71\,500\ \mathrm{N\,mm^{-2}}$ and $\nu = 0.33$. The single point × is for a plate 100 mm square and 1.0 mm thick with $E = 306\,000\ \mathrm{N\,mm^{-2}}$ and $\nu = 0.25$, and a loading circle diameter of 25.0 mm. $d_l/2a$: ●, 0.25; ■, 0.075; ×, 0.25.

It is assumed that, following the Timoshenko indicator, the geometric linearity limit depends only on δ_c/t, irrespective of the elastic constants of the material. Support for this stance is given by a single calculation for an alumina plate (E ca. five times that of aluminium and $\nu = 0.25$) 1 mm thick with $d_l/2a = 0.25$ and $d_s/2a = 1.41$. The value of δ_c/t for this case is seen to fall close to the curve in Fig. 6 for aluminium plates. It is therefore concluded that Fig. 6 can be used for all plates irrespective of elastic constants.

In order to apply the criterion $\delta_c \leqslant 0.5$ for the validity of the linear solution for the load–stress relation, it is necessary to be able to calculate what the central deflection will be with a particular material and for a particular loading geometry. The means of achieving this end is presented in the next section.

5. Results of the linear analysis of the plate stresses and deflections

The conditions at the centre of the plate are concentrated on, where the stresses are very close to the maximum stress in the plate which occurs on the loading circle and therefore close to the stress at the point at which fracture is nucleated.

For geometrically linear conditions, the stresses are pure bending throughout the plate (neglecting shear stresses) and, at the centre, the moment per unit length is independent of the elastic modulus and the plate thickness; it varies slightly with Poisson's ratio, ν. For a particular value of ν, the centre moment/unit length is given by

$$M_c = AP$$

where P is the applied load. The maximum tensile stress at the plate centre is then given by

$$\sigma_c = \frac{M_c(t/2)}{I}$$

where t is the plate thickness and I, the second moment of area per unit width of the plate, is

$$I = \frac{t^3}{12}$$

So

$$\sigma_c = \frac{6M_c}{t^2}$$

The value of A depends on the loading geometry, i.e. $d_l/2a$ and $d_s/2a$. Fig. 7 shows how the centre moment/unit length/unit load (A) varies with the loading ring diameter for a particular corner support location.

Table IV lists values of A calculated by finite element analysis for $\nu = 0.25$ and 0.33. A is dimensionless (its units are $\mathrm{N\,mm\,mm^{-1}\,N^{-1}}$).

The data in Table IV make it possible to predict the load required to generate a particular stress at the centre of the plate given the plate thickness and loading geometry. If the selected stress is the estimated

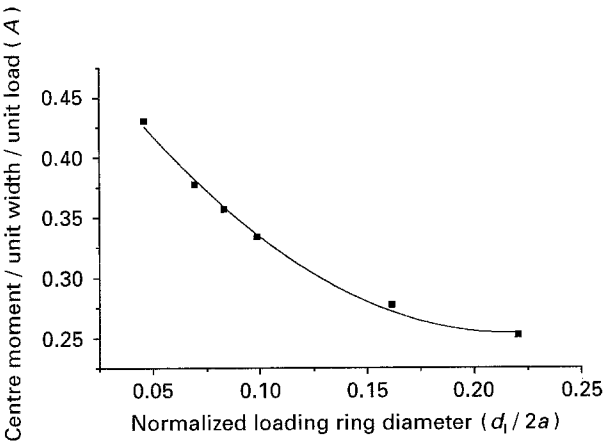

Figure 7 Graph showing the variation of moment at the centre of a plate with loading ring diameter. These are measured values. The tests were carried out on a duralumin plate 254 mm square and 9.82 mm thick with supports at $d_s/2a = 1.378$.

TABLE IV Values of A in the relation $M_c = AP$ for two values of Poisson's ratio and for selected values of loading ring diameter and support positions

$d_l/2a$	$d_s/2a$	A	
		$\nu = 0.25$	$\nu = 0.33$
0.25	1.414	0.228	0.234
	1.000	0.164	0.171
	0.850	0.140	0.146
	0.700	0.114	0.120
0.075	1.414	0.350	0.364
	1.000	0.286	0.300
	0.850	0.261	0.275
	0.700	0.236	0.248

fracture stress of the plate material then the calculated load will be close to the fracture load of the plate because the centre stress is close to the maximum stress in the plate.

It is then necessary to judge if this load will produce plate deflections within the geometrically linear regime so that the linear solution for the load–stress relationship can be used to find the fracture stress from the fracture load. The following data give that information.

The general theory of plate bending [4] suggests that the central deflection of a loaded plate will be given by

$$\delta_c = k\frac{Pa^2(1-\nu^2)}{Et^3} \quad (1)$$

where $2a$ is the length of the side of the square plate, and k will depend on the loading and supporting geometry. Values of k for a range of geometries are listed in Table V.

The value of the central deflection of the plate, δ_c, produced by an estimated or measured fracture load P can be obtained by selecting the appropriate value of k from Table V and substituting it in Equation 1 for δ_c together with the plate dimensions and the elastic constants. If the value of δ_c/t turns out to be less than

TABLE V Values of k in the relation $\delta_c = kPa^2(1-\nu^2)/Et^3$ for selected values of loading ring diameter and support positions

$d_l/2a$	$d_s/2a$	k	$d_l/2a$	$d_s/2a$	k
0.25	1.414	1.730	0.075	1.414	1.883
	1.000	0.585		1.000	0.656
	0.850	0.368		0.850	0.430
	0.700	0.213		0.700	0.268

0.5 then the linear solution can be used to determine the fracture stress from the fracture load P.

6. An example of the application of the data

The aim is to establish if it is legitimate to use the results of the linear analysis to calculate the fracture stress from the fracture load in the following circumstances.

The specimens are glass plates 100 mm square and 3.5 mm thick. The elastic modulus is 70 GN m^{-2} and Poisson's ratio is 0.22. The support points lie on a circle 85 mm in diameter, so $d_s/2a = 0.85$. The more critical case of the largest loading circle diameter is taken. This is 25 mm so $d_l/2a = 0.25$. The estimated fracture stress is 150 N mm^{-2}. The centre moment needed to generate this stress at the centre of the plate on the lower surface is

$$M_c = \frac{\sigma_c t^2}{6} = \frac{150 \times 3.5^2}{6} = 306.25 \text{ N mm mm}^{-1}$$

From Table IV, the appropriate value of A is 0.138, so the load needed to generate M_c is

$$P = \frac{M_c}{A} = \frac{306.26}{0.138} = 2219 \text{ N}$$

The central deflection produced by this load is

$$\delta_c = k\frac{Pa^2(1-\nu^2)}{Et^3}$$

From Table V, $k = 0.368$, so

$$\delta_c = \frac{0.368 \times 2219 \times 50^2(1-0.22^2)}{70\,000 \times 3.53} \text{ mm}$$

$$= 0.647 \text{ mm}$$

and

$$\frac{\delta_c}{t} = \frac{0.647}{3.5} = 0.185$$

This is below the critical value of 0.5, so the linear analysis can be used for this test condition.

7. The distribution of the maximum tensile principal stress on the lower plate surface in the linear regime

Figs 8 and 9 give the radial distribution for plates 100 mm square of the maximum moment/unit length/unit load (A) for directions 0, 15, 30 and 45° from the line joining the mid-point of the opposite

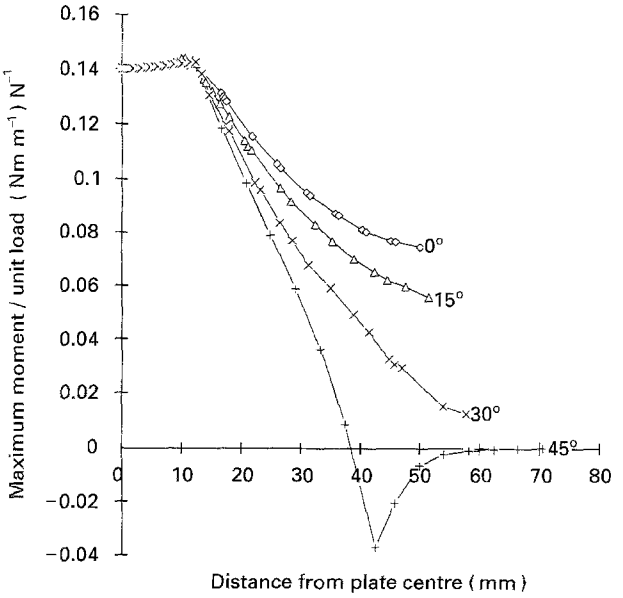

Figure 8 The radial variation of the maximum bending moment at a point for four values of θ, the polar coordinate of the point relative to the line joining the mid-point of the opposite sides of the plate as zero. $d_1/2a = 0.25$, $d_s/2a = 0.85$.

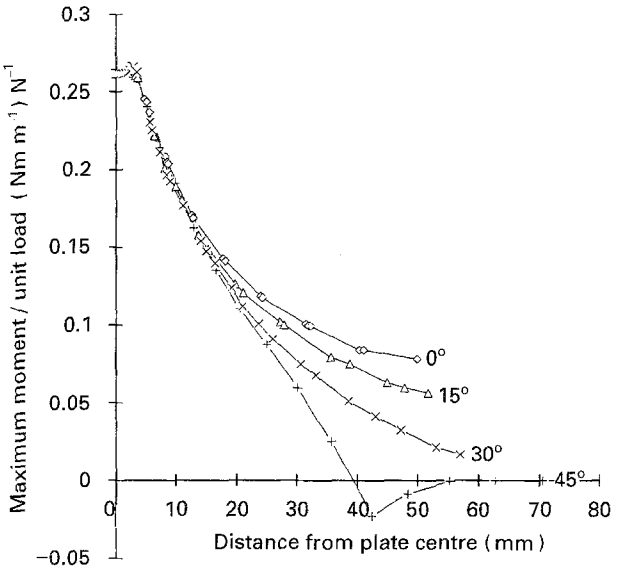

Figure 9 As for Fig. 8 with $d_1/2a = 0.075$.

sides of the plate. So, 45° is the direction of a plate diagonal joining opposite plate corners. The data are for $d_1/2a = 0.25$ and 0.075, and for $d_s/2a = 0.85$, which is the recommended corner-support position for fracture testing. The calculations used a value for Poisson's ratio of 0.25. Table VI tabulates the data for easier reference.

For general interest, Figs 10 and 11 show comparable data for $d_s/2a = 1.334$, i.e. for conditions where the corner supports are quite close to the plate corners, and Figs 12 and 13 are contour plots of the distribution of moment/unit length/unit load (A) over a quarter of the plate for $d_s/2a = 0.85$.

To determine the fracture stress at the fracture origin from the measured fracture load, P_f, first locate the polar coordinates of the fracture origin (r, θ), where r is

TABLE VI Values of the maximum moment/unit length/unit load (A) at the point $(r/2a, \theta)$

$r/2a$	A			
	$\theta = 0$	$\theta = 15°$	$\theta = 30°$	$\theta = 45°$
$d_1/2a$=0.25; ν = 0.25				
0	0.1401	0.1401	0.1401	0.1401
0.025	0.1403	0.1403	0.1403	0.1402
0.05	0.1406	0.1409	0.1408	0.1408
0.075	0.1413	0.1418	0.1416	0.1414
0.10	0.1417	0.1439	0.1420	0.1423
0.125	0.1421	0.1422	0.1426	0.1427
0.135	0.1410	0.1379	0.1372	0.1349
0.14	0.1375	0.1358	0.1342	0.1319
0.15	0.1362	0.1320	0.1292	0.1267
0.16	0.1330	0.1285	0.1251	0.1217
0.17	0.1298	0.1251	0.1211	0.1169
0.18	0.1264	0.1220	0.1170	0.1123
0.19	0.1230	0.1189	0.1130	0.1079
0.20	0.1205	0.1159	0.1091	0.1026
0.225	0.1141	0.1122	0.0986	0.0910
0.25	0.1085	0.1009	0.0885	0.0785
0.275	0.1024	0.0943	0.0805	0.0662
0.30	0.0972	0.0882	0.0730	0.0540
0.325	0.0926	0.0823	0.0656	0.0405
0.35	0.0885	0.0772	0.0560	0.0255
0.40	0.0819	0.0687	0.0462	
0.45	0.0773	0.0626	0.0341	↑
0.50	0.0750	0.0575	0.0240	Negative
0.515		0.0559		moment
0.577			0.0128	↓
$d_1/2a$=0.075; ν = 0.25				
0	0.2615	0.2615	0.2615	0.2615
0.01	0.2615	0.2615	0.2616	0.2616
0.02	0.2616	0.2621	0.2620	0.2619
0.03	0.2619	0.2636	0.2665	0.2614
0.035	0.2597	0.2605	0.2625	0.2593
0.04	0.2550	0.2550	0.2550	0.2545
0.05	0.2450	0.2400	0.2400	0.2460
0.06	0.2325	0.2265	0.2265	0.2310
0.07	0.2215	0.2150	0.2150	0.2185
0.08	0.2115	0.2045	0.2045	0.2075
0.09	0.2010	0.1940	0.1940	0.1965
0.10	0.1920	0.1850	0.1850	0.1865
0.125	0.1720	0.1655	0.1655	0.1655
0.15	0.1550	0.1495	0.1495	0.1470
0.175	0.1425	0.1360	0.1360	0.1300
0.20	0.1320	0.1245	0.1245	0.1140
0.25	0.1160	0.1080	0.0980	0.0890
0.30	0.1035	0.0940	0.0790	0.0600
0.35	0.0930	0.0805	0.0625	0.0258
0.40	0.0855	0.0710	0.0480	
0.45	0.0800	0.0635	0.0345	↑
0.50	0.0785			Negative
0.518		0.0568		moments
0.53			0.0217	↓

the distance from the centre of the plate and θ is the angle measured from the nearest line joining the mid-point of opposite sides of the plate. Express r in terms of the plate side length $2a$, $r/2a$, and from Table VI establish, by linear interpolation, the value A_f of the moment/unit load/unit length (A) at that point. The fracture stress will be given by

$$\sigma_f = \frac{6A_fP_f}{t^2}$$

where t is the plate thickness.

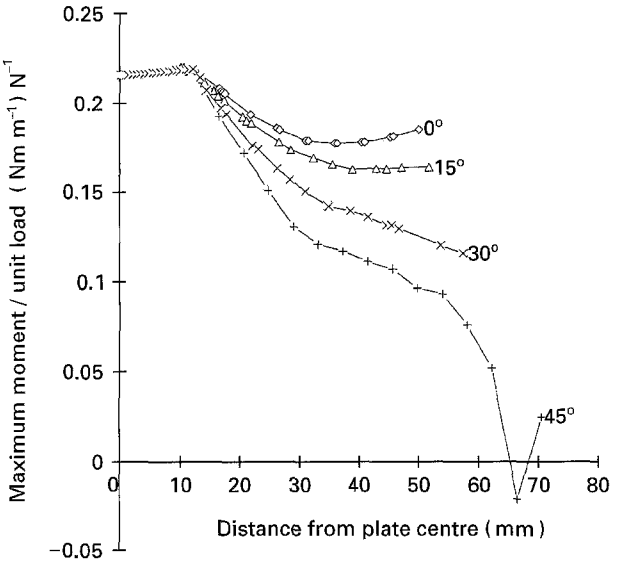

Figure 10 As for Fig. 8 but with the corner supports near the plate corner, $d_s/2a = 1.334$ and $d_l/2a = 0.25$.

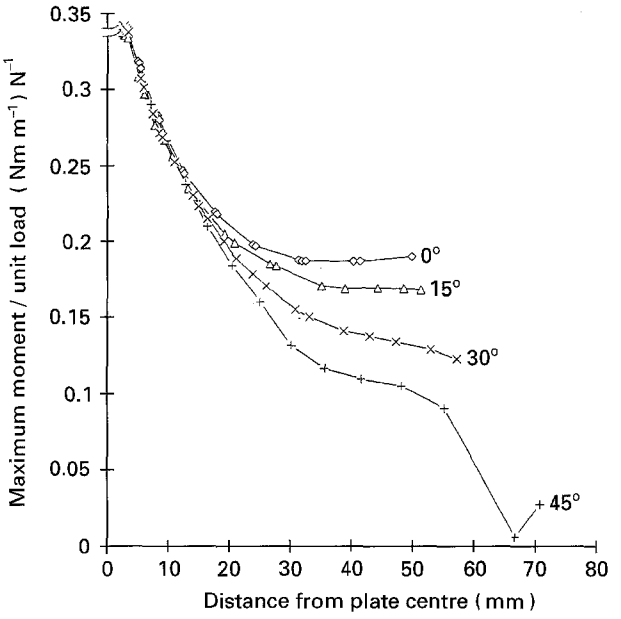

Figure 11 As for Fig. 10 but with $d_l/2a = 0.075$.

The data in Table VI are calculated for a value of Poisson's ratio of 0.25. An adequate correction for a different value of ν can be secured by assuming that the effect of Poisson's ratio on the stress determined by the procedure now described is proportionally the same as the effect on A (which is proportional to the centre stress) in Table IV.

The following example illustrates the procedure for the determination of the fracture stress. The specimen is a square plate with a side length ($2a$) of 150 mm and thickness 3 mm; it fractured at a load of 1605 N, and the fracture origin lay at $r = 19.5$ mm and $\theta = 20°$. The loading diameter was 37.5 mm, corresponding to $d_l/2a = 0.25$; $r/2a = 19.5/150 = 0.130$. From Table VI, interpolation between $r/2a = 0.125$ and $r/2a = 0.135$ and between $\theta = 15°$ and $\theta = 30°$ gives $A_f = 0.140$. The bending moment/unit length at the fracture origin was therefore

$$M_f = 0.140 \times 1605 = 224.7\,\text{N mm mm}^{-1}$$

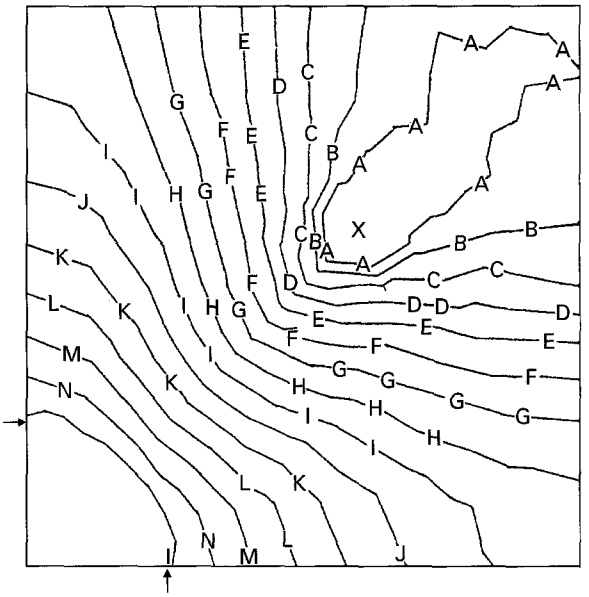

Figure 12 A contour plot of the variation over a quarter of the plate of the maximum bending moment. The contours connect points of constant bending moment/unit width/unit load (A). The arrows indicate the loading ring position and X is a support point. $d_l/2a = 0.25$ and $d_s/2a = 0.85$. Contour values: A, 0; B, 0.01; C, 0.02; D, 0.03; E, 0.04; F, 0.05; G, 0.06; H, 0.07; I, 0.08; J, 0.09; K, 0.10; L, 0.11; M, 0.12; N, 0.13; O, 0.14; P, 0.15.

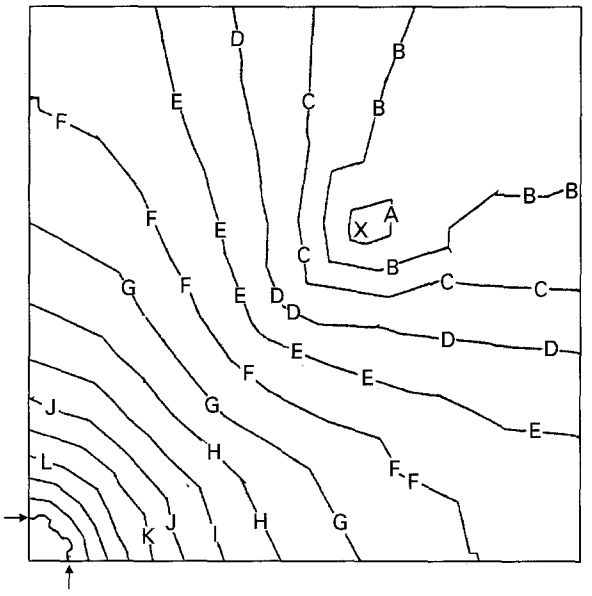

Figure 13 As for Fig. 12 but with $d_l/2a = 0.075$. Contour values: A, 0.01295; B, 0.06477; C, 0.02590; D, 0.04533; E, 0.06476; F, 0.08419; G, 0.1036; H, 0.1230; I, 0.1425; J, 0.1619; K, 0.1813; L, 0.2008; M, 0.2202; N, 0.2396; O, 0.2590.

and the corresponding surface tensile stress at that point was

$$\sigma_f = \frac{6 \times 224.7}{3^2} = 149.8\,\text{N mm}^{-2}$$

which is the fracture stress for the plate.

8. The effect of stressed volume on the average fracture stress

An advantage of the concentric loading arrangement is that the effective stressed volume of the plate is

easily changed by changing the diameter of the loading circle. It is helpful to know the effective stressed volume for plates loaded in this manner in order, for example, to explore if Weibull statistics predict observed volume dependence. It has been demonstrated [1] that since fracture is initiated at the tensile stressed surface, the effective surface area is an acceptable alternative to effective volume.

The effective area of this tensile face, A_{A2}, is defined as: $A_{A2} = K_{A2}A_0$, where A_0 is the total area of this face of the plate ($= (2a)^2$), and

$$K_{A2} = \sum_{i=1}^{N} \left(\frac{\sigma_{i1}^m + \sigma_{i2}^m}{\sigma_p^m} \right) \frac{\Delta A_i}{A_0}$$

where σ_{i1} and σ_{i2} are the two principal stresses in the plane of the plate at the ith Gauss point, and σ_p is the maximum tensile principal stress in the whole plate; m is the Weibull modulus. ΔA_i is the area associated with the ith Gauss point and is obtained by dividing the area of the element in which the Gauss point is located by the number of Gauss points in the element. Values of K_{A2} are tabulated in Table VII for $d_l/2a = 0.075$ and 0.25, and for $d_s/2a = 0.85$ – the support position recommended for fracture testing. Geometrical linearity has been assumed and data are presented for two values of Poisson's ratio, 0.25 and 0.33. The values are independent of the elastic modulus of the material.

It is worth noting that the values of K_{A2} are very sensitive to the precision with which the peak stress in the plate, σ_p, is determined. For example, a 3% error in σ_p produces a 55.8% error in σ_p^m when $m = 15$ and will change K_{A2} by 55.8%.

TABLE VII Values of K_{A2} in the relation $A_{A2} = K_{A2}A_0$, where A_0 is the total area of the lower face of the plate and A_{A2} is the effective area. Calculated for support positions $d_s/2a = 0.85$ and for two values of Poisson's ratio. Assumes geometrical linearity

Weibull modulus, m	K_{A2}	
	$\nu = 0.25$	$\nu = 0.33$
$d_l/2a$=0.25		
4.5	0.162	0.152
5.0	0.146	0.138
5.5	0.133	0.126
6.0	0.122	0.116
6.5	0.113	0.108
7.0	0.105	0.101
7.5	0.0978	0.0943
10.0	0.0730	0.0715
12.5	0.0572	0.0567
15.0	0.0461	0.0461
$d_l/2a$=0.075		
4.5	0.0338	0.0315
5.0	0.0286	0.0267
5.5	0.0247	0.0232
6.0	0.0217	0.0204
6.5	0.0194	0.0183
7.0	0.0175	0.0166
7.5	0.0160	0.0152
10.0	0.0112	0.0107
12.5	0.00861	0.00832
15.0	0.00696	0.00677

TABLE VIII The effect of shear on the centre deflection and the centre moment of concentrically loaded plates of different thickness; $d_s/2a$, 0.85; $d_l/2a$, 0.25; E, 360 GN m^{-2}; ν, 0.25

Plate thickness (mm)	δ_c with shear / δ_c with shear ignored	M_c with shear / M_c with shear ignored
1	1.000	0.997
6	1.041	1.000
10	1.113	1.000
15	1.254	1.006
20	1.500	1.008

8.1. The effect of shear stresses

As the thickness of the plate increases relative to the plate side length, shear stresses develop which are distributed parabolically across the plate thickness and are zero at the plate surfaces.

The plate thickness at which shear stresses begin to have an effect on the centre moments and the centre deflection of loaded plates was investigated using the ABAQUS package. Table VIII lists the ratio of the central deflection to that with shear ignored and correspondingly for the centre moment/unit length/unit load (A).

The calculations were carried out for a plate 100 mm square with a 25 mm loading circle and supported at points lying on a circle 85 mm in diameter, corresponding to $d_s/2a = 0.85$. The value of E was 360 GN m^{-2} and ν was 0.25. The load was 200 N, but for this linear case the ratios will be independent of load.

So, for the loading configuration recommended for fracture testing, the effect of shear on the centre moments, and therefore on the tensile stresses in the central region of the plate, can be ignored for values of the plate thickness less than 1/5 of the length of the side of the plate. In contrast, significant effects of shear on the deflection arise if the plate thickness exceeds 1/20 of the length of the side of the plate.

Acknowledgements

The author is grateful to Professor John Humphreys for the provision of laboratory and computational facilities. Thanks also to Professor F. M. Burdekin for making the ABAQUS finite element expertise of his research group in the Department of Civil and Structural Engineering in UMIST freely available through Drs Dong Mei Qi and Sabi Al-Lahan. Dr Richard Day gave valuable help with the LUSAS package, as did Dr David Hall with various computational tasks.

References

1. K. M. ENTWISTLE, *J. Mater. Sci.* **26** (1991) 1078.
2. *Idem., ibid.* **28** (1993) 2007.
3. C. J. SMITHELLS (ed.) "Metals reference book", 4th Edn (Butterworths, London, 1967) p. 708.
4. S. P. TIMOSHENKO and S. WOINOWSKY-KRIEGER, "Theory of plates and shells", 2nd Edn (McGraw Hill, Singapore, 1959) p. 48.

Received 14 November 1994
and accepted 15 March 1995